Biophysical Journal Volume 71 August 1996 1024–1035

Increased Work in Cardiac Trabeculae Causes Decreased Mitochondrial NADH Fluorescence Followed by Slow Recovery

Rolf Brandes and Donald M. Bers
Loyola University Medical Center, Department of Physiology, Maywood, Illinois 60153 USA

ABSTRACT The oxidative phosphorylation rate in isolated mitochondria is stimulated by increased [ADP], resulting in decreased [NADH]. In intact hearts, however, increased mechanical work has generally not been shown to cause an increase in [ADP]. Therefore, increased [NADH] has been suggested as an alternative for stimulating the phosphorylation rate. Such a rise in [NADH] could result from stimulation of various substrate dehydrogenases by increased intracellular [Ca^{2+}] (e.g., during increased pacing frequency). We have monitored mitochondrial [NADH] in isolated rat ventricular trabeculae, using a novel fluorescence spectroscopy method where a native fluorescence signal was used to correct for motion artifacts. Work was controlled by increased pacing frequency and assessed using time-averaged force. At low-pacing rates (~0.1 Hz), [NADH] immediately decreased during contraction and then slowly recovered (~5 s) before the next contraction. At higher rates, [NADH] initially decreased by an amount related to pacing rate (i.e., work). However, during prolonged stimulation, [NADH] slowly (~60 s) recovered to a new steady-state level below the initial level. We conclude that 1) during increased work, oxidative phosphorylation is not initially stimulated by increased mitochondrial [NADH]; and 2) increased pacing frequency slowly causes stimulation of NADH production.

INTRODUCTION

The myocardium has the ability to match its energy supply to demand. During increased cardiac work and ATP consumption rate, the rate of oxygen consumption is raised because of an increased rate of oxidative phosphorylation. This increased rate also requires an increased rate of substrate dehydrogenation, producing the reduced form of mitochondrial nicotinamide adenine dinucleotide (NADH). NADH, in turn, provides the electron transport chain with electrons necessary to build the proton motive force, ultimately regenerating ATP from ADP and P_i.

If increased work caused increased [ADP], then ADP itself may provide a regulatory signal to enhance the rate of oxidative phosphorylation. In isolated mitochondria addition of ADP causes an increased oxidative phosphorylation rate (Jacobus et al., 1982; Koretsky et al., 1987). However, during increased work in intact hearts, [ADP] appears to be unchanged (Katz et al., 1987; From et al., 1986) or to increase (From et al., 1986) depending on the substrate used. It, therefore, seems unlikely that ADP is the only control signal for oxidative phosphorylation. Alternatively, increased NADH/NAD^+ redox state has been suggested as a control factor in the up-regulation of oxidative phosphorylation in vivo (Balaban and Heineman, 1989). According to this mechanism, a rise in NADH/NAD^+ would accompany increased work as shown by Katz et al. (1987). In this case, the problem is to find the control signal(s), which may stimulate substrate oxidation (NADH production) during increased work so as to raise NADH/NAD^+.

Fig. 1 shows a simple flow diagram summarizing the hypothesis. During increased work, a stimulus may up-regulate NADH production causing NADH/NAD^+ to rise. Such an increase may, for example, be mediated by increased mitochondrial Ca^{2+}, which has been shown to stimulate mitochondrial dehydrogenases in isolated preparations (Hansford, 1991; McCormack et al., 1990; Crompton, 1990). The increased NADH/NAD^+ may subsequently stimulate oxidative phosphorylation. If this is the major factor in early adjustments to increased work, it should result in a rapid and maintained elevation of NADH/NAD^+.

We have extended the pioneering work of Chance et. al. (1965) by developing a new, noninvasive method of reliably measuring NADH/NAD^+ in intact cardiac trabeculae using fluorescence spectroscopy. The goals of the current study were 1) to determine if NADH/NAD^+ does indeed rise during increased work (i.e., supporting the hypothesis above), and 2) to evaluate a possible role of Ca^{2+} in stimulating substrate oxidation to increase the NADH production rate.

Using fluorescence spectroscopy to assess NADH/NAD^+ and time-averaged isometric force to assess for ATP-hydrolysis rate (work) it was found that 1) NADH/NAD^+ decreased during increased work, indicating that it is not the main early activator of oxidative phosphorylation, and suggesting that there is another control signal; and 2) the NADH production rate was slowly stimulated during a prolonged increase in work where average cytosolic Ca^{2+} was expected to increase. This is consistent with the idea of Ca^{2+} stimulation of mitochondrial dehydrogenase activity in vivo. This stimulation was not sufficient, however, to fully compensate for the work-dependent decrease of NADH/NAD^+.

Received for publication 8 November 1995 and in final form 24 April 1996.
Address reprint requests to Dr. Rolf Brandes, Loyola University Medical Center, Department of Physiology, 2160 South First Avenue, Maywood, IL 60153. Tel.: 708-216-5599; Fax: 708-216-6308; E-mail: rbrande@luc.edu.

0006-3495/96/08/1024/12 $2.00

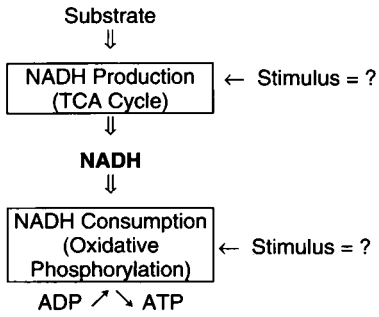

FIGURE 1 Simplified flow diagram illustrating mitochondrial NADH production via tricarboxylic acid cycle (TCA) and consumption via oxidative phosphorylation.

METHODS

Trabeculae isolation and mounting

The preparation of trabeculae was similar to that reported previously by Backx and Ter Keurs (1993). Brown male LBN-F1 rats (370–510 g) were deeply anesthetized and anticoagulated by injecting 65 mg pentobarbital and 1000 U heparin intraperitoneally. The heart was excised by midsternal thorocotomy, quickly arrested by placing it in iced, modified Krebs-Henseleit solution, and then perfused at ~28°C using the Langendorff method. The modified Krebs-Henseleit solution contained (in mM): NaCl (108), KCl (21), $MgCl_2$ (1.2), $CaCl_2$ (0.5), $NaHCO_3$ (24), Glucose (4), sodium pyruvate (10), insulin (20 units/L); and was equilibrated with a 95% O_2, 5% CO_2 gas mixture to produce pH = 7.40 (±0.05) at 24°C. In experiments involving hypoxia, a 95% N_2, 5% CO_2 gas mixture was used instead.

The heart was dissected at ~28°C by carefully cutting the right ventricular free wall along the septum and around the aorta, and removing the right atrium, thus freeing the tricuspid valve. Trabeculae running from the tricuspid valve (attached by connective tissue) to the free wall or the septum were carefully removed by cutting off a piece of the surrounding valve at one end and a piece of the surrounding free wall (carnal) at the other end. The trabeculae were band-shaped with a cross-sectional area of 0.058 ± 0.024 mm^2, and a minor axis of 0.16 ± 0.02 mm, which is expected to be small enough to allow adequate oxygen diffusion to the center of the trabeculae (Snow and Bressler, 1977). Initial developed force, at $[Ca^{2+}]_o$ = 2 mM, was 48 ± 5 mN/mm^2 (4.9 ± 0.5 g/mm^2).

After dissection, the muscle was transferred to and mounted in a muscle chamber, paced at 0.5 Hz (Grass S44, Grass Instruments, Quincy, MA), and superfused at 15 ml/min (Rabbit peristaltic pump, Rainin Inc., Woburn, MA) with the Krebs-Henseleit solution described above, except that instead of 21 mM, 6 mM KCl was used, and T = 24°C. A vacuum line was attached to the opposite end of the muscle chamber to remove the perfusate. To measure muscle force, a specially designed basket in the muscle chamber held the carnal end of the trabeculae and was glued onto a piezoresistive force transducer (AE875, Aksjeselskapet Micro-Elektronikk, Horten, Norway) that was mounted on a micromanipulator (see Fig. 2). The signal from the transducer was amplified (Gould Incorporated, Cleveland, Ohio), digitized, and stored in a PC (see below). The valve end was hooked onto a stainless steel needle attached to another micromanipulator, which was used to set the desired muscle (sarcomere) length. Two platinum wires (each ~1-cm-long) were positioned parallel to and ~1 mm away from the trabeculae for field stimulation. The voltage was adjusted to 1.5 times the voltage needed for threshold activation (typically ~5 volts).

The trabeculae were allowed to equilibrate for 15–30 min at 0.5 Hz before the perfusion solution was changed from 0.5 to 2 mM Ca^{2+} (defined as standard solution) and stretched to produce maximum isometric developed force.

Fluorescence measurements

Fig. 2 shows the instrumental design used for the NADH fluorescence measurements. The excitation light source contained a 150-W Xenon arc lamp, an ultraviolet-reflecting dichroic mirror (not shown) and an infrared-absorbing filter (Oriel Corporation, Stratford, CT). Excitation at 350 nm was obtained using an interference filter (bandwidth 10 nm; Chroma Technologies, Brattleboro, VT). A shutter and neutral density filters (not shown) were used to minimize UV exposure (Oriel Corporation, Stratford,

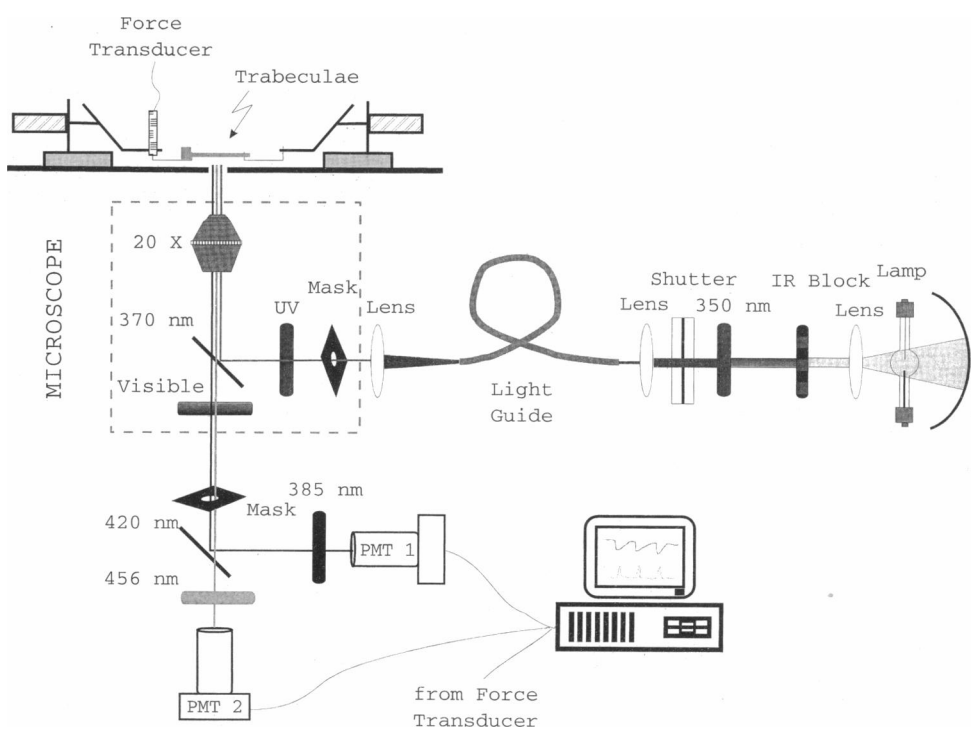

FIGURE 2 Instrumental design (see text).

CT). Excitation light was passed, using a liquid light guide (Oriel Corporation, Stratford, CT), to a Nikon Diaphot inverted microscope equipped with a 20X Fluor objective (Nikon, Tokyo, Japan), and directed on the trabeculae by a dichroic mirror (370-nm long-pass; Chroma Technologies, Brattleboro, VT). Instrumental autofluorescence was minimized by using ultraviolet and visible transmitting filters (ChromaTechnologies, Brattleboro, VT) in combination with masks that allowed restriction of the illumination and detection areas. A dichroic mirror (420-nm long-pass; Reynard Corporation, San Clemente, CA) reflected short wavelength light through a 385-nm interference filter (nominally 390 nm, bandwidth 22 nm; Chroma Technologies, Brattleboro, VT) and onto a photomultiplier tube (Oriel Corporation, Stratford, CT). Light transmitted through the 420-nm mirror was usually filtered by a 456-nm interference filter (nominally 460 nm, bandwidth 10 nm; Chroma Technologies, Brattleboro, VT) and directed onto a second photomultiplier tube. The emission wavelengths were chosen to minimize fluorescence intensity changes due to changes in tissue light absorbance (Brandes et al., 1994) and motion artifacts (Brandes et al., 1992). The specified wavelengths of the interference filters were obtained by slightly tilting them with regard to the incoming beam.

In experiments involving a reference dye, light at a third emission wavelength was simultaneously detected by using a second 500-nm, long-pass dichroic mirror (Corion, Holliston, MA) placed immediately after the 420-nm dichroic mirror (not shown). Emitted light at 456 nm was, in this case, reflected by the 500-nm mirror, and light at 550 nm was transmitted and further filtered by an interference filter at 550 nm (bandwidth 30 nm; Chroma Technologies, Brattleboro, VT) before being detected by a third photomultiplier tube (not shown).

The signals from the photomultiplier tubes were amplified (Oriel Corporation, Stratford, CT) and digitized simultaneously with the force transducer signal by an analog-to-digital board (ATI-MIO16F-5; National Instruments, Austin, Texas) and data acquisition software (MicroCal Software Incorporated, Northampton, MA) at a rate of 200 samples/s, analog low-pass filtered at 100 Hz, and stored in a PC (Dell Dimension XPS P90; Dell Corporation, Roundrock, TX) for later analysis.

Light transmission measurements

The instrumental configuration for the transmission experiments was similar to the fluorescence configuration. Instead of ultraviolet excitation, the built-in light source of the microscope (50-W Halogen) was used to irradiate the trabeculae from above. The microscope diaphragm and condenser were used to limit exposure to a circular area ~1 mm in diameter. Transmitted light was further masked to allow detection of only light that had passed through the muscle, and the intensity was adjusted by neutral density filters. The 420-nm dichroic mirror was replaced by a plate beamsplitter (Reynard Corporation, San Clemente, CA), and interference filters at 440 and 456 nm were used (10-nm bandwidths; Chroma Technologies, Brattleboro, VT). These wavelengths were chosen because hypoxia was expected to change the tissue light transmission at 440 nm but not at 456 nm (because 456 nm is a myoglobin isosbestic wavelength) (Brandes et al., 1994).

Elimination of motion artifacts

The motion artifact in the NADH sensitive fluorescence at 456 nm was eliminated by detecting fluorescence emission at a second wavelength that was less sensitive to changes in [NADH]. Two different methods were used to obtain a reference signal: 1) by using native muscle fluorescence at a wavelength where NADH fluorescence is comparatively small, or 2) by measuring the fluorescence from a fluorescent dye that had been used to stain the muscle.

The reference signal was corrected by eliminating any NADH-sensitive component (see below), and a corrected fluorescence ratio (Ratio) was calculated by dividing the signal at 456 nm by the corrected reference signal.

Native reference

In isolated mitochondria, the NADH-dependent emission intensity at 385 nm is much smaller than at 456 nm (<16%) (Koretsky et al., 1987); however, relative to the weak non-NADH-dependent fluorescence at 385 nm in an intact heart, it may still be significant. A method was, therefore, developed whereby the relative NADH contribution at 385 nm was first determined and then used to mathematically correct the reference signal to make it insensitive to changes in [NADH]. The relative NADH contribution was determined by suddenly stopping the electrical stimulation because this caused characteristic changes in [NADH] while the trabeculae were not moving (see Results). The slope of the relationship between the signals at 456 and 385 nm, during the rest phase, was then used to mathematically correct the reference signal (see Appendix).

Dye reference

A reference dye signal at 550 nm was obtained by loading the trabeculae with a reference dye. The trabeculae were perfused with standard solution containing 0.05 mg/ml of 5-(and-6)-carboxy-2′,7′-dichlorofluorescein diacetate, succinimidyl ester (Molecular Probes, Eugene, OR) for ~15 min. This dye permanently stains the trabeculae and has previously been used as a reference signal to eliminate motion artifacts in connection with NADH measurements (Heineman and Balaban, 1993). Residual dye was washed away for at least 20 min or until the reference signal was stable. Typically, the fluorescence at 550 nm increased fourfold after dye loading. Because of the small loading factor, the dye reference signal was corrected in a manner similar to the native reference signal.

NADH redox state

The fluorescence technique does not allow direct determination of the NADH redox state, because only NADH, but not NAD^+, is fluorescent. However, to compare the mitochondrial NADH/NAD^+ ratio in this work with others, the common definition was used (see Appendix):

$$\mathrm{NADH/NAD^+} = \qquad (1)$$

$$(\mathrm{Ratio^c_{ctrl}} - \mathrm{Ratio^c_{min}}) / (\mathrm{Ratio^c_{max}} - \mathrm{Ratio^c_{min}})$$

where $\mathrm{Ratio^c_{ctrl}}$ is the (corrected) fluorescence ratio measured during control conditions, $\mathrm{Ratio^c_{min}}$ is the Ratio during application of a mitochondrial uncoupler, carbonyl cyanide P-(trifluoromethoxy) phenylhydrazon (FCCP) (Sigma Chemical Company, St. Louis, MO), and $\mathrm{Ratio^c_{max}}$ is the Ratio during application of a mitochondrial inhibitor, sodium cyanide (Aldrich Chemical Company, St. Louis, MO). At the end of each experiment, the inhibitor (cyanide; 5 mM) and uncoupler (FCCP; 2 μM) were separately applied in sequence to the trabeculae using perfusion solutions that were otherwise identical to the standard perfusate. A simpler method to inhibit oxidative phosphorylation was also attempted by eliminating the substrates, pyruvate and glucose, from the perfusion solution (which was otherwise identical to the standard).

Assessment of ATP hydrolysis rate and data analysis

The time-averaged force was used as an index of work related ATP hydrolysis rate. This indirect and simplified measure assumes that the ATP hydrolysis rate is related to active force during the whole (isometric) contraction cycle. (Cooper, 1979). A 0.2-Hz low-pass filter was applied to the force signal to obtain average force by using software digital filtering (MicroCal Software Incorporated, Northampton, MA). The signal-to-noise ratio of the fluorescence ratio was similarly improved by a 3-Hz digital low-pass filter. Results were reported as means ± SE. Statistical analysis

was performed using Student's t-test (paired where applicable), and differences were considered significant when $p < 0.05$.

RESULTS

Correction of reference signal

Fig. 3 *A* shows the force and fluorescence signals from a trabecula during rest and when paced at 3 Hz. During pacing and afterwards at rest, the fluorescence intensities changed with time, both at 385 nm (reference) and 456 nm (NADH), although the intensity variations with regard to noise were larger at 456 nm than at 385 nm. This variation in intensity is expected to arise from changes in [NADH] and from motion artifacts (Brandes et al., 1992). To use the 385-nm reference signal to correct the 456-nm NADH signal for motion artifacts, the NADH component of the 385-nm signal was first removed using the following technique.

Fig. 3 *B* shows the raw data from Fig. 3 *A*, plotted with the intensity at 385 nm versus the intensity at 456 nm. During stimulation, the intensity relationship between the signals at the two wavelengths depends on motion artifacts and changes in [NADH]. After pacing at rest, however, the relationship is determined exclusively by the relative NADH signal contribution at 385 vs. 456 nm, provided that [NADH] is changing (a single point would otherwise result). For example, if there is no NADH contribution at 385 nm, the relationship would be described by a line with slope = 0. Fig. 3 *B* shows that during rest, slope = 0.05. Fig. 3 *A* shows the effect of correcting the reference signal by mathematically eliminating the NADH contribution using the slope and the signal at 456 nm (see Appendix, Eq. A4a). The intensity variation in the corrected reference signal at 385 nm is mainly due to motion artifacts. Note that the overshoot, upon cessation of stimulation, is absent in the corrected reference signal but not in the original (raw) reference signal. The corrected reference signal illustrates the intrinsic assumption that there is no motion artifact at rest, despite the changes in the raw reference signal.

It should be noted that the fluorescence intensities at both detection wavelengths were found to slowly decrease over several hours and at different rates (Ashruf et al., 1995). Consequently, the slope may slowly change during the total experimental protocol, typically 4–5 h. Accurate correction during the whole experimental protocol therefore requires repeated determination of the slope.

An NADH signal, independent of motion artifacts, was obtained by dividing the 456-nm signal with the corrected 385-nm reference signal to obtain a fluorescence ratio. To determine the effects of using an incorrect slope (e.g., because of changes during the experimental protocol), the Ratio was also calculated using the uncorrected, raw signal (i.e., incorrectly assuming slope = 0). Fig. 3 *A* shows the calculated Ratio using either the 385-nm signal before correction (Raw Ratio) or after correction (Corr Ratio). In both cases, the ratio calculation eliminated the motion transients observed at 456 nm during stimulation. The main difference in using the corrected reference was that the corresponding Ratio was larger overall. However, the time dependency of the Ratios were qualitatively similar in both cases. This is further illustrated in Fig. 3 *C* where the two ratios were normalized so that the minimum and maximum intensities coincided. Fig. 3 *C* shows that the qualitative changes in the NADH signal were independent of correcting the reference. Therefore, proper correction of the reference would be important for quantitative purposes, but unimportant for elimination of motion artifacts and evaluation of qualitative changes in [NADH].

Slow time-dependent changes in [NADH]

Fig. 3 *C* shows complex phasic changes of the Ratio, and therefore of [NADH], upon stimulation and cessation of

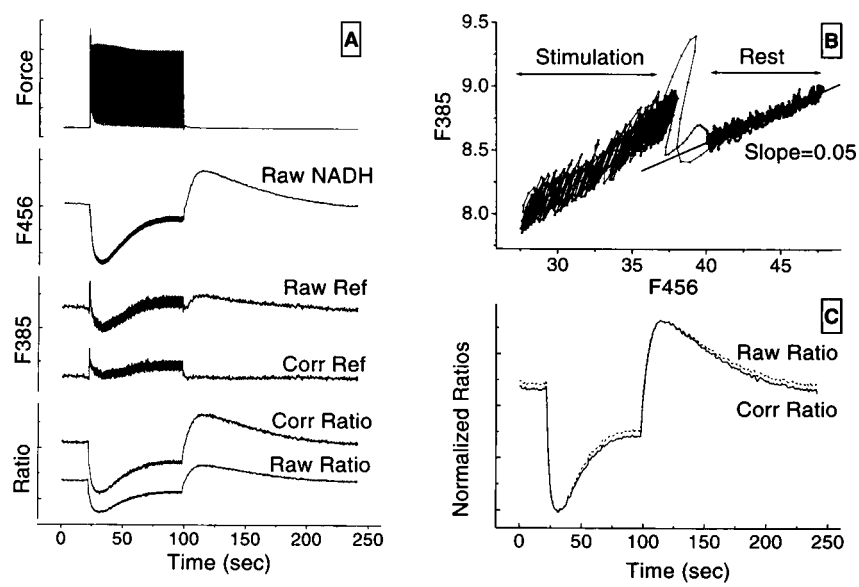

FIGURE 3 Fluorescence signals and calculation of corrected fluorescence ratio when a trabecula was at rest, paced at 3 Hz, and then resting again. *A*. Force (*top trace*), fluorescence emissions at 456 nm (F456; Raw NADH), 385 nm before correction (F385, Raw Ref) and after correction (F385, Corr Ref). Fluorescence ratio using F385 before correction (Raw Ratio) and using corrected reference (Corr Ratio). *B*. Determination of slope (see text) using same data as in *A*, with uncorrected F385 plotted versus F456. *C*. Comparison of normalized Ratios obtained using uncorrected reference (Raw Ratio; *dotted line*) and corrected reference (Corr Ratio; *solid line*).

stimulation. When the muscle was stimulated, the fluorescence ratio immediately decreased below resting level to reach a minimum in ~5 s. The Ratio then partially recovered to a new lower steady-state level after ~60 s of stimulation (creating an apparent initial undershoot). When stimulation ceased, the Ratio rose above original resting level (overshoot), and then slowly returned to the initial level (during ~2–3 min). The magnitude of this overshoot depended on stimulation time and frequency. If stimulation was interrupted after ~5 s, the ratio initially decreased and then returned to resting levels without any apparent undershoot or overshoot. The same qualitative changes were observed in all muscles studied ($n > 20$), although the magnitude of the under- and overshoot varied.

Muscle oxygenation

A possible explanation of the recovery from a minimum to a new steady-state level during the undershoot could be due to inadequate muscle oxygenation during prolonged stimulation. As a consequence, the oxidative phosphorylation rate would decrease and cause [NADH] to slowly increase. When stimulation ceased the oxygen deficiency could remain, causing [NADH] to overshoot until oxygen had diffused into the core of the muscle during the rest period. To investigate the possibility of oxygen deficiency, experiments were performed to evaluate the myoglobin oxidation state.

Fig. 4 *A* shows the force and light transmission through a 0.21-mm-thick trabecula at steady-state stimulation (1 Hz). After the perfusion solution was switched from one saturated with O_2 to one saturated with N_2, the muscle slowly (~60 s) became hypoxic as evidenced by the drop in force and decreased light transmission at 440 nm, whereas it was unchanged at 456 nm (myoglobin isosbestic wavelength) (Brandes et al., 1994). Upon returning to the O_2-containing solution, force and light transmission returned to initial values.

Fig. 4 *B* shows the force and fluorescence emission at 456 and 440 nm, using the same protocol as above. During hypoxia, the fluorescence intensity at 456 nm increased as expected because of inhibited oxidative phosphorylation and consequently increased [NADH]. In contrast, at 440 nm the fluorescence intensity was constant, which incorrectly gave the impression that [NADH] was constant. The result at 440 nm can be explained by the offsetting effects of decreased light transmission (because of increased myoglobin light absorption) and increased fluorescence intensity (because of increased [NADH]).

Fig. 4 *C* shows the force and light transmission both when the muscle was resting and when stimulated at 3 Hz. In contrast to the effect of hypoxia, neither force nor light transmission changed during prolonged stimulation. There was, however, a sudden decrease in light transmission at both 440 and 456 nm, and an increase in the transmission ratio immediately after the onset of stimulation. These sudden intensity changes at both wavelengths can be explained by a motion artifact, because hypoxia took many seconds to develop and had more profound effects on the light transmission at 440 nm than at 456 nm. Note that in contrast to the fluorescence ratio, a transmission ratio may not cancel motion artifacts.

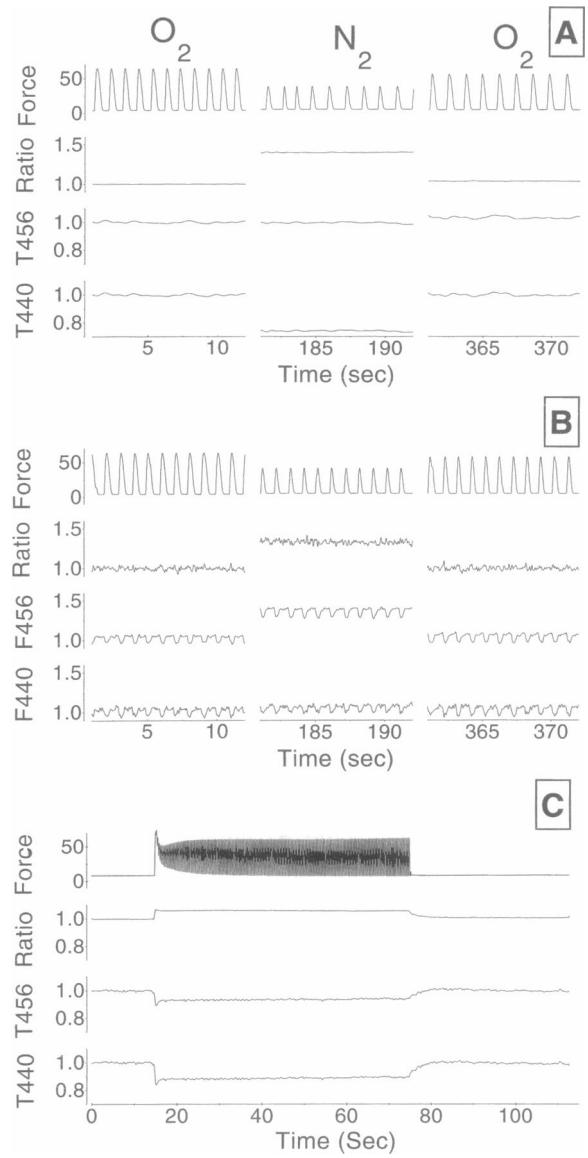

FIGURE 4 Comparison between hypoxia and high frequency pacing on force, light transmission at 456 and 440 nm (T456 and T440, respectively), fluorescence (F456 and F440, respectively) and calculated ratios. The light transmission signals were time averaged to suppress high frequency fluctuations due to motion artifacts. Control condition using 95% O_2, 5% CO_2 (O_2) and hypoxia using 95% N_2, 5% CO_2 (N_2). *A*. Effect of hypoxia on light transmission. *B*. Effect of hypoxia on fluorescence. *C*. Effect of prolonged pacing at 3 Hz on light transmission.

Because there was no progressive decline in either force or light transmission at 440 nm during prolonged stimulation, it can be concluded that the observed under- and overshoot in the fluorescence ratio cannot be explained by hypoxia.

Beat-to-beat changes in [NADH]

Fig. 5 shows time-resolved force and fluorescence intensity variations when the trabecula was first paced at 0.1 Hz, and then at 1 Hz. The upward deflection of the fluorescence traces coincides with force development, and can be attributed to motion artifacts. Immediately after contraction (at 0.1 Hz), the NADH sensitive emission at 456 nm decreased below resting level, and then slowly (~5–10 s) recovered. In contrast, the corrected reference emission at 385 nm, showed no variation after contraction. The calculated Ratio demonstrates excellent suppression of the motion artifact, and demonstrates that the [NADH] falls immediately during the contraction, and then slowly recovers. When the pacing frequency was increased to 1 Hz, the Ratio still showed beat-to-beat fluctuations and the average Ratio level decreased. This behavior was observed in all preparations studied ($n > 20$), although the time constant of recovery after contraction varied among preparations, and even within a preparation during the ~4-h-long experimental protocol.

Increased pacing rates cause decreased [NADH]

Fig. 6 shows the effects of changing pacing frequency on the force and fluorescence ratio. In the example shown in Fig. 6, *A* and *B*, the trabecula had been loaded with the reference dye and two different reference signals were simultaneously detected at 385 and 550 nm.

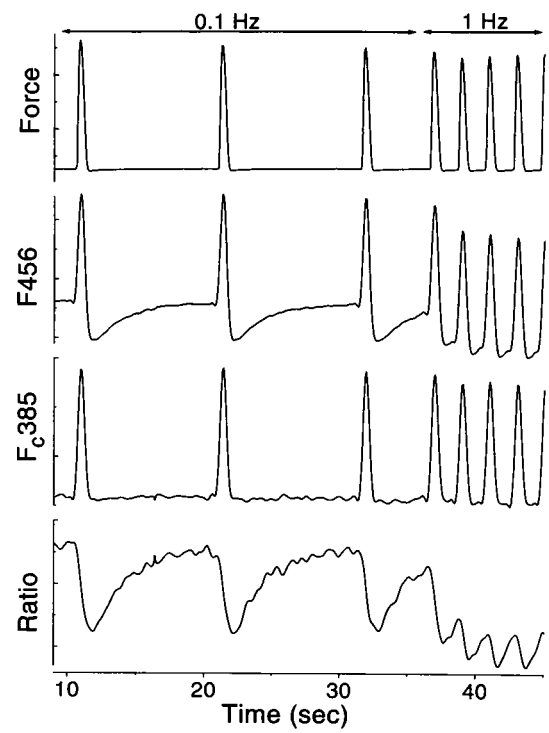

FIGURE 5 Beat-to-beat changes in Ratio ([NADH]) when pacing at 0.1 and 1 Hz. [NADH] was assessed, and motion artifact eliminated by calculating a ratio between fluorescence at 456 nm (F456) and corrected fluorescence at 385 nm (F_c385).

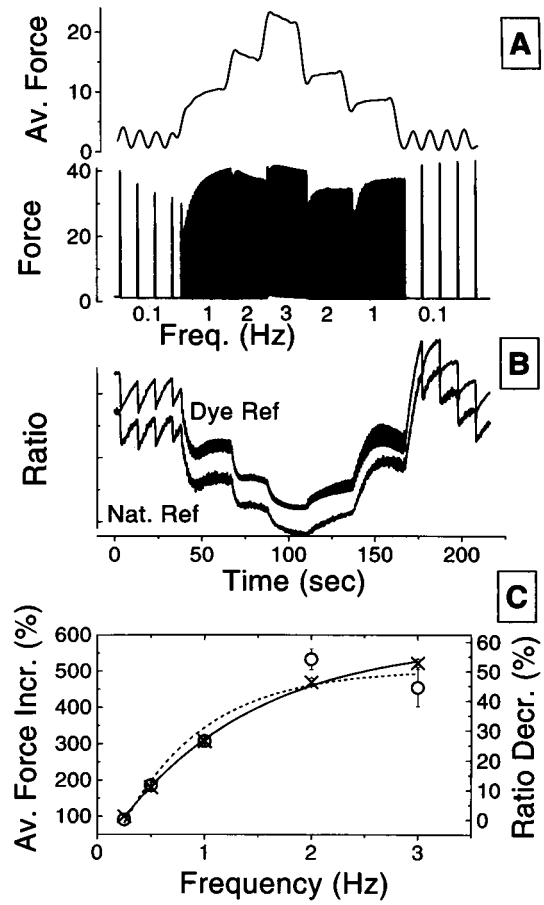

FIGURE 6 Increased pacing rates cause increased average force and decreased fluorescence ratio. In the example (*A* and *B*), the trabecula was loaded with a fluorescent dye. *A*. Time-averaged force (Av. Force; *top trace*) and force (*bottom trace*). Units are in mN/mm^2. *B*. Reference signals (not shown) were obtained simultaneously at 385 nm (native fluorescence) and 550 nm (dye fluorescence). Both reference signals were corrected to eliminate the NADH fluorescence contribution before calculating the ratio between the emission at 456 nm and dye reference (Dye Ref) or native reference (Nat. Ref). *C*. Pooled data ($n = 5$) from trabeculae without dye when pacing at 0.25, 0.5, 1, 2, and 3 Hz. Fluorescence ratio values obtained immediately after onset of stimulation (minimum values). Force (*cross*) and Ratio (*open circle*) are shown relative to 0.25 Hz, which was normalized to unity. Lines (*solid* for force and *dashed* for Ratio) were obtained by fitting data points to exponential association functions.

Fig. 6 *A* shows that when pacing frequency was increased, resting and peak force did not change significantly. Time-averaged force, however, increased as a function of pacing frequency up to 3 Hz. If the frequency was increased greater than 3 Hz, average force fell because of incomplete activation (resulting in alternans, and/or missing beats). The average force did not show any hysteresis if pacing frequency was increased from 0.1 to 3 Hz, and then decreased from 3 to 0.1 Hz.

Fig. 6 *B* shows the effect of changing pacing frequency on the fluorescence ratio. The Ratio was calculated by using either the corrected native reference signal at 385 nm or the

corrected dye reference signal at 550 nm. At a frequency of 0.1 Hz, the previously noted beat-to-beat changes in the Ratio ([NADH]) were observed. As the frequency was increased from 0.1 to 1 Hz corresponding to increased average force, the Ratio fell; this trend continued as frequency was further increased to 2 and 3 Hz. When the frequency was reduced corresponding to decreasing average force, the Ratio increased again and eventually returned to control level. The Ratio showed some hysteresis, especially noticeable by comparing the Ratio at the beginning of the protocol (0.1-Hz pacing rate) with the Ratio at the end of the protocol (0.1 Hz). This hysteresis is closely related to the overshoot shown previously in Fig. 3. The observed results were identical whether the native reference signal or the dye signal was used to calculate the Ratio. (Note that in Fig. 6, there were smaller incremental changes in pacing frequency and the duration at any given frequency was shorter than in Fig. 3, consequently, there was less apparent under- and overshoot in Fig. 6 than in Fig. 3.)

Fig. 6 *C* shows pooled fluorescence and average force data as a function of pacing frequency at 0.25, 0.5, 1, 2, and 3 Hz (using trabeculae without a reference dye). With increasing frequency, average force increased and the Ratio (i.e., [NADH]) fell. [NADH] is, therefore, negatively correlated with the average force or work related ATP hydrolysis rate.

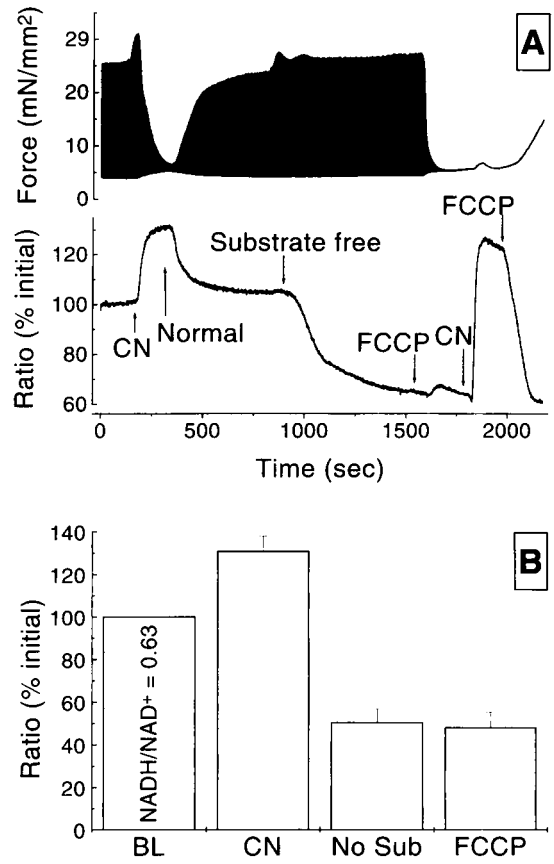

FIGURE 7 Calculation of NADH redox state, NADH/NAD$^+$. *A*. Force and fluorescence ratio while pacing at 1 Hz, starting with normal perfusate and applying: Cyanide (CN, 5 mM, to maximally reduce NAD$^+$), normal, substrate free (to maximally oxidize NAD$^+$), FCCP (2 μM, attempting to oxidize NAD$^+$ further), cyanide again (to maximally reduce NAD$^+$ again), and FCCP (to maximally oxidize NAD$^+$ again). *B*. Pooled data from (n = 6) experiments as in *A*. Perfusion with normal perfusate (BL) normalized to 100%, maximum NAD$^+$ reduction (CN), NAD$^+$ oxidation by eliminating substrate (No Sub), and maximum NAD$^+$ oxidation using FCCP (FCCP).

NADH redox state

Fig. 7 *A* shows a typical Ratio calibration trace used to determine the NADH/NAD$^+$ ratio at 1-Hz pacing frequency. The trabecula was initially perfused with standard solution (baseline; BL). To maximally reduce NAD$^+$, the standard solution was switched to the cyanide solution, which caused the Ratio to increase immediately (by 30%) while peak force slowly fell. When the Ratio had reached a new steady-state level, the standard solution was returned, causing the Ratio and force to slowly return to control levels. To maximally oxidize NAD$^+$, two different solutions were used. The standard solution was first replaced by the substrate-free solution, resulting in a slowly decreasing Ratio, but the force remained constant. When the Ratio had reached a new steady-state level, the substrate-free solution was switched to one containing the mitochondrial uncoupler (FCCP). The addition of FCCP caused an immediate drop in peak force, but the Ratio did not decrease to a lower value than when substrate-free solution was used.

If FCCP was only briefly applied (~4 min) and cyanide was reapplied, the maximum Ratio was once again obtained, and it was only slightly lower than initially. Reapplication of FCCP caused the Ratio to again reach a minimum, and resting force gradually increased (rigor development due to ATP depletion).

Fig. 7 *B* shows pooled data (n = 6). When NAD$^+$ was maximally reduced, the Ratio rose 31 ± 3% above control, and when NAD$^+$ was maximally oxidized, the Ratio dropped to 49 ± 3% of control. There was no statistical difference between using substrate-free solution or FCCP to determine the minimum Ratio. NADH/NAD$^+$ was individually calculated using Eq. 1 for each experiment of the type in Fig. 6 *A*, and for all muscles NADH/NAD$^+$ = 0.63 ± 0.03 (at 1-Hz pacing frequency).

DISCUSSION

We have developed a new method to assess the redox state of mitochondrial NADH in intact cardiac trabeculae using NADH fluorescence spectroscopy. Using this approach, our main finding was that cardiac muscle contraction caused decreased mitochondrial NADH/NAD$^+$, both within a contraction cycle and as a function of stimulation frequency. This decrease of [NADH] occurred despite the observed slow activation of NADH production (recovery) during prolonged stimulation.

Use and correction of a reference signal

NADH fluorescence spectroscopy is intrinsically sensitive to motion of the tissue and it is therefore necessary to correct for motion artifacts. Motion artifacts are typically minimized by using a fluorescent reference signal at a wavelength where NADH fluorescence is minimal. Because motion is expected to modulate the NADH and reference fluorescence intensities similarly, a ratio between them would minimize motion artifacts (Brandes et al., 1992).

Two different approaches to obtain a reference signal have been employed previously. In the first approach, the tissue was loaded with a fluorescent dye either by immersing the tissue in dye-containing solution (Heineman and Balaban, 1993) or by coronary perfusion with dye-containing solution (Brandes et al., 1992; Brandes et al., 1994). In the second approach, a second detection wavelength was used where the native heart fluorescence was relatively insensitive to changes in [NADH] (White and Wittenberg, 1993).

There are two main disadvantages of using a reference dye. First, it is practically difficult to apply the dye, and it would prolong any experimental protocol. Second, the application of the dye may change tissue viability and/or the tissue physiology so that experimental results may be unreliable. In our hands, we found that loading the trabeculae with the reference dye sometimes caused decreased muscle force and reduced viability. In the thin trabeculae used here, the whole tissue was loaded. Thus, any functional impairment due to the dye would be more pronounced than when only the surface of whole hearts is loaded (Heineman and Balaban, 1993).

Fig. 6 demonstrated that, in a viable preparation loaded with a reference dye, the experimental results were identical whether the native or an exogenous dye signal was used as a reference. We therefore conclude that a native reference signal is preferable to a dye reference as it is more practical and less invasive.

Fig. 3 demonstrated that the NADH fluorescence intensity contribution at the reference wavelength could be eliminated from the reference signal by first determining the relationship (slope) between the NADH and reference signals, and then correcting the reference signal. To investigate the importance of correcting the reference, the fluorescence ratio was calculated with and without correction of the reference signal. Although the absolute value of the fluorescence ratio differed in these two cases, the qualitative aspects of the time dependency of the Ratio were indistinguishable. Repeated determinations of the slope and correction of the reference signal may therefore be important for quantitative purposes (e.g., determination of NADH/NAD^+), but would not greatly affect the time dependency of the NADH signal within a single protocol.

Dual wavelength emission detection, using a native fluorescence reference at 415 nm and calculating a difference rather than a ratio, has been reported previously using isolated myocytes (White and Wittenberg, 1993). However, a difference signal is not expected to be a very efficient method of suppressing motion artifacts (Brandes et al., 1992), and calculating a ratio would result in a noisy signal, because the NADH fluorescence is still relatively large at 415 nm. Alternatively, an NADH ratio may be obtained by excitation at two different excitation wavelengths, although this also causes incomplete cancellation of motion artifacts (unless, as the authors demonstrated, corrected by mathematical means) (Scott et al., 1994).

Work- and time-dependent changes in [NADH]

Because oxygen consumption was not measured directly in this study, an assessment of work-related ATP hydrolysis rate had to be made from the measured force. In intact contracting hearts, Yasumura et al. (1989) suggested that the majority of ATP hydrolysis occurs as peak force develops, with little hydrolysis during the relaxation phase. Therefore, the hydrolysis rate may in this case be assessed from the product of developed force and frequency. However, in isometrically contracting trabeculae, a linear relationship between energy consumption and the force-time integral has been has been demonstrated (Cooper, 1979), making the use of time-averaged force a reasonable index of ATP hydrolysis rate or work. Recalculation of some experimental data using the force-frequency product produced qualitatively similar results (data not shown). Consequently, we have chosen to use the time-averaged force rather than the force-frequency product.

Beat-to-beat changes in [NADH]

Fig. 5 demonstrated the variation of [NADH] within a stimulation cycle (beat-to-beat changes), and this has also been demonstrated previously in papillary muscle (Chapman, 1972). However, we believe that our study more accurately represented the true variation in [NADH] because motion artifacts were suppressed using a fluorescent reference rather than a reflected light reference. The latter method eliminates motion artifacts relatively poorly (Brandes et al., 1992). In contrast, in a recent study using cardiac cells, no beat-to-beat changes were observed (White and Wittenberg, 1993), and this may be because of the lower workload in unloaded isolated myocytes versus the isometrically contracting trabeculae in this study.

The beat-to-beat changes are consistent with stimulation of NADH consumption by ADP, which would, in this case, need to increase during a single contraction. However, phosphate metabolites and ADP have been shown to be constant during the cardiac cycle (Koretsky et al., 1983; Kantor et al., 1986) in situ. This is in contrast to the glucose-perfused heart where PCr and ATP were shown to vary during the contraction cycle (Fossel et al., 1980). It is possible that the work here was lower than the work in situ so that ADP may be limiting in our case (see Study Limitations and Possible Sources of Artifacts, below). In this

case, beat-to-beat regulation by ADP may occur in contrast to the in situ situation.

Another explanation would be the possibility of beat-to-beat Ca^{2+} activation of the mitochondrial ATP synthase (Doumen et al., 1995) without a corresponding instantaneous increase in the activation of the mitochondrial dehydrogenases. Further studies are needed to evaluate if transient increases in work at constant $[Ca^{2+}]_i$ also cause a transient drop in [NADH].

Increased pacing rates cause decreased [NADH]

Figs. 3 *C* and 6 demonstrated that when average force was increased by increased pacing frequency, [NADH] fell correspondingly. Increased pacing rate results in an increased flux of reducing equivalents from substrate through the tricarboxylic acid cycle to produce NADH and in an increased rate of oxidative phosphorylation (which consumes NADH). A fall of mitochondrial [NADH] is expected only if the production rate of NADH is not increased in proportion to match the consumption rate.

Production of NADH may be regulated by key mitochondrial enzymes such as pyruvate dehydrogenase, oxoglutarate dehydrogenase complexes and NAD-linked isocitrate dehydrogenase (McCormack et al., 1990; Crompton, 1990). In vitro and in isolated mitochondria, increased $[Ca^{2+}]$, [ADP], and [ADP]/[ATP] have each been shown to stimulate the NADH production rate (McCormack et al., 1990; Crompton, 1990). It has therefore been suggested that increased pacing rate preferentially stimulates NADH production versus consumption rate, which would raise [NADH] (and thereby stimulate the oxidative phosphorylation rate) (Balaban and Heineman, 1989). The opposite was found here; and oxidative phosphorylation cannot, therefore, be controlled by increased [NADH] (at least not during the initial frequency-dependent changes reported here).

Our results are similar to an early study using rabbit papillary muscle, where [NADH] decreased at the onset of pacing from rest (Chapman, 1972). Isolated cardiac cells, have also been used to demonstrate decreasing [NADH] with increasing pacing frequency, although the time constant for NADH changes was much longer (several minutes), and only occurred at frequencies approaching 5 Hz (White and Wittenberg, 1993). The weaker response may have been due to the lower workload in unloaded isolated myocytes versus the isometrically contracting trabeculae in this study.

In contrast, studies using intact hearts have yielded contradictory results regarding a possible role of NADH as a control signal for oxidative phosphorylation (Katz et al., 1987; Heineman and Balaban, 1993; Ashruf et al., 1995). In the first study (Katz et al., 1987), [NADH] increased with increasing pacing frequency, although this may have been an artifact due to hypoxia resulting from inadequate coronary flow at high pacing rates (Heineman and Balaban, 1993). In the second study, [NADH] remained constant when pacing frequency was increased (Heineman and Balaban, 1993), but the lack of a decrease may again have been caused by partial hypoxia (Ashruf et al., 1995). In the most recent study (Ashruf et al., 1995), [NADH] decreased with increasing pacing rates as observed in the present study.

Slow time-dependent changes in [NADH]

Fig. 3 *C* demonstrated that the NADH signal initially fell at the onset of pacing and recovered partially during prolonged pacing. Upon cessation of pacing, [NADH] overshot the resting level and then slowly returned. The slow recovery and overshoot suggest a slow mechanism that first activates and then deactivates NADH production. An overshoot similar to ours has also been observed in rabbit papillary muscle, although the authors regarded this as an "indication of metabolic disturbances, occurring less than 25% of the time" (Chapman, 1972). In contrast, we always observed the undershoot and overshoot using our protocol (in more than 20 muscles).

Study limitations and possible sources of artifacts

Work regime

Previous investigators have pointed out that the regulatory mechanisms of oxidative phosphorylation may differ depending on work regime (From et al., 1990). For example, at very low work levels [ADP] may be limiting and control the oxidative phosphorylation rate. However, as work is increased by a large amount, [ADP] may no longer be limiting and the oxidative phosphorylation rate may instead be controlled by [NADH] (From et al., 1990). It would therefore be useful to know where the muscle is working with regard to its maximum capacity or to the in vivo situation.

At 24°C the maximum work in our studies was obtained at 3 Hz because the muscles would not follow higher pacing frequencies at this temperature. Fig. 6 showed that the NADH fluorescence monotonically decreased with work over a wide range of work, from the minimum at 0.25 Hz up to the maximum at 3 Hz where work had increased fivefold. In working rat hearts at 37°C, From et al. (1990) found O_2 consumption rates of 0.15 and 0.21 $\mu mol \cdot g^{-1} \cdot contraction^{-1}$ at 5 and 3 Hz, respectively. This is not very different from estimates by Cooper (1979) in cat papillary muscle at 0.5 Hz and 29°C (0.12 $\mu mol \cdot g^{-1} \cdot contraction^{-1}$). Therefore, the work/contraction in intact hearts and the trabeculae studied here may not be very different. Of course, further studies are needed at increased pacing rates (and temperature) to extend the results obtained in this study to more physiological conditions.

Temperature

A low temperature (24°C) was used in this study to slow down the kinetics such that any stimulation of NADH

production would be more easily observable. At a higher temperature, faster kinetics of increased NADH production and consumption might obscure the under- and overshoot. However, if the Q_{10} of NADH production is larger than muscle ATPase activity, then increased temperatures (e.g., 37°C) may result in less of a decrease of [NADH] with work than was observed here. It would therefore be valuable to extend the results obtained here to higher, more physiological temperatures.

Mitochondrial NADH fluorescence contribution

The fluorescence arising from cells may, in principle, have contributions from NADH and NADPH localized in cytosol or mitochondria. However, in hearts perfused with glucose, it has been estimated that ~80% of the heart fluorescence (at 447 nm) originates from mitochondrial NADH (Eng et al., 1989). In our study pyruvate was used, which would raise the mitochondrial NADH contribution even more because glycolysis is reduced. We therefore conclude that mitochondrial NADH fluorescence dominates over mitochondrial NADPH and cytosolic NAD(P)H.

It should be cautioned however, that the intensity of the NADH fluorescence intensity would be affected by a change in fluorescence quantum yield. It has, for example, been suggested that application of uncouplers may change the mitochondrial environment (swelling), thereby altering the quantum yield (Balaban and Mandel, 1988; Ji et al., 1979). Furthermore, early work has demonstrated an inverse relationship between uncoupler concentration and fluorescence intensity (enhancement) (Estabrook et al., 1963). However, in this study, $NADH_{min}$ was identical whether substrate-free perfusion or FCCP was used. Additionally, $NADH_{max}$ could be obtained again if cyanide was reapplied after brief perfusion with FCCP. It is possible that the brief exposure to FCCP in this study was not long enough to cause major environmental changes to NADH in the mitochondria. Consequently, no substantial change in NADH fluorescence quantum yield is expected in vivo. (Longer exposure to FCCP before reapplication of cyanide caused decreased $NADH_{max}$; not shown).

Motion artifacts

Fig. 5 demonstrated that a large motion artifact in the NADH signal was effectively suppressed by calculating the Ratio. Even if a small artifact was hidden in the rapid downstroke, the NADH level remained lower than during rest long after the mechanical contraction, and therefore motion, has ceased. We therefore believe that our results and conclusions were not affected by motion artifacts.

Muscle oxygenation

Inadequate muscle oxygenation during increased pacing rates may cause two possible complications: 1) It would change the myoglobin absorption spectrum, thereby artifactually altering fluorescence intensities (Brandes et al., 1994; Fralix et al., 1990). This artifact can be avoided by using detection at isosbestic wavelengths as was done in this study (Brandes et al., 1994). 2) Inadequate oxygenation would also inhibit oxidative phosphorylation causing a rise in [NADH], and this could explain the recovery and overshoot. It is, however, unlikely that the trabeculae would become hypoxic because of its small size (cross-section 0.16 mm) versus much larger (~1 mm) papillary muscles where oxygenation was not limiting (Snow and Bressler, 1977).

Nevertheless, we measured the myoglobin light absorption and found that it was unaffected by pacing, in contrast to the changes observed during hypoxia. Furthermore, force remained constant during stimulation, in contrast to the decline observed during hypoxia. We therefore conclude that our results were not affected by oxygen deficiency.

Fig. 4 *B* also demonstrated the importance of proper choice of detection wavelength. If myoglobin nonisosbestic wavelengths were used (e.g., 440 nm, or a long-pass filter) changes in [NADH] could be distorted because of changes in myoglobin absorption, emphasizing the importance of using isosbestic wavelengths (e.g., 456 nm) for NADH fluorescence studies during hypoxia (Brandes et al., 1994; Fralix et al., 1990).

Muscle pH

Acidification to ~pH 6.3 results in decreased NADH fluorescence intensity (White and Wittenberg, 1993), and this could explain the apparent decrease in [NADH] during increased pacing rates. However, there is no reason to expect decreased pH under our conditions (White and Wittenberg, 1993; Katz et al., 1987).

NADH redox state

Fig. 7 demonstrated that the $NADH/NAD^+$ ratio was 0.63 at 24°C, a pacing rate of 1 Hz, and in the presence of pyruvate and 2 mM Ca^{2+}. Our value was higher than those obtained in glucose perfused preparations (at 37°C). For example, in intact rat hearts paced at 5 Hz, $NADH/NAD^+ \sim 0.26$ (at 1.75 mM $[Ca^{2+}]$) (Scott et al., 1994), and in resting myocytes, $NADH/NAD^+$ was 0.27 (White and Wittenberg, 1993). This difference may be explained by the inclusion of pyruvate in this study, as pyruvate has been shown to increase $NADH/NAD^+$ (Laughlin and Heineman, 1994; Ashruf et al., 1995), by the dependency of $NADH/NAD^+$ on work (Fig. 6), and possibly by our lower temperature.

Another effect of using high pyruvate concentration is the expected strong activation of pyruvate dehydrogenase, rendering the enzyme potentially less sensitive to further activation by Ca^{2+} (Kobayashi and Neely, 1983). If the recovery and overshoot is indeed caused by Ca^{2+} activation of mitochondrial dehydrogenases, it is therefore plausible that the sites of activation are at the oxoglutarate dehydrogenase complexes or NAD-linked isocitrate dehydrogenase.

Further studies are needed to investigate if the results presented in this study could be reproduced at lower NADH/NAD^+ ratios (e.g., by manipulating substrate and/or temperature).

Summarizing model

Increased pacing frequency, and consequently ATP hydrolysis rate, may be expected to cause increased average cytosolic (and possibly mitochondrial) [Ca^{2+}], [ADP], and/or [ADP][P_i]/[ATP]. Initially, increased [ADP] and/or [ADP][P_i]/[ATP] may have stimulated respiration (NADH consumption) causing decreasing [NADH] (Crompton, 1990). Simultaneously, increased [ADP]/[ATP] may have stimulated NADH production by activating mitochondrial dehydrogenases (Crompton, 1990). However, the stimulation of NADH production was less than the stimulation of NADH consumption because NADH/NAD^+ decreased.

A second regulatory mechanism was subsequently evoked as evidenced by the slow NADH recovery during prolonged stimulation. This could be caused by increased activation of the mitochondrial dehydrogenases, and may have been a result of increased mitochondrial [Ca^{2+}] or lowered NADH/NAD^+ ratio (Crompton, 1990).

When pacing ceased, the primary stimulation of NADH production and consumption was quickly eliminated, but the secondary stimulation of the NADH production remained, causing [NADH] to overshoot. As Ca^{2+} left the mitochondria or the increased NADH/NAD^+ ratio caused inhibition of the enzymes, the secondary stimulation ceased and [NADH] returned to the initial level.

The model suggested above is consistent with results from isolated mitochondria, where increased [ADP] has been shown to up-regulate the oxidative phosphorylation rate causing decreased [NADH] (Koretsky et al., 1987). It is also consistent with results from whole pyruvate perfused hearts where increased pacing rates caused increased [ADP] and [ADP][P_i]/[ATP] (From et al., 1986), decreased [NADH] (Ashruf et al., 1995), and increased mitochondrial [Ca^{2+}] in cardiac myocytes (Di Lisa et al., 1993).

Furthermore, the time constants of the recovery and overshoot (~30 s) were similar to mitochondrial Ca^{2+} uptake and efflux times in intact myocytes (Bassani et al., 1993) and to the experimentally or mathematically found time constants for Ca^{2+}-dependent activation of mitochondrial enzymes (Crompton, 1990). This is consistent with the possibility that the recovery and overshoot may be caused by slow Ca^{2+}-dependent activation and inactivation of mitochondrial dehydrogenases.

APPENDIX

Correction of reference signal

After subtraction of instrumental autofluorescence, the fluorescence intensities (F385 and F456) at the two detection wavelengths, 385 and 456 nm, respectively, can be described according to:

$$F385 = (BG_{385} + [NADH] \cdot A_{385}) \cdot m(t) \quad (A1)$$

$$F456 = (BG_{456} + [NADH] \cdot A_{456}) \cdot m(t) \quad (A2)$$

where BG_{385} and BG_{456} are the muscle background, non-NADH-dependent, fluorescence intensities at respective detection wavelength, [NADH] is the NADH concentration, A_{385} and A_{456} are constants related to the NADH fluorescence quantum yield (fluorescence magnitude at wavelengths 385 and 456 nm, respectively), and $m(t)$ is a motional modulation function caused by movement of the trabeculae with regard to the light source and detection system (Brandes et al., 1992). When the muscle is at rest ($m(t) = 1$), Eqs. A2 and A1 can be combined to eliminate the dependency on [NADH]:

$$F385 = BG_{385} + (F456 - BG_{456}) \cdot A_{385}/A_{456} \quad (A3)$$

According to Eq. A3, F385 is expected to be linearly dependent on F456, with slope = A_{385}/A_{456}. This slope (e.g., measured at rest in Fig. 3 *B*) can be used to calculate a corrected reference signal, F_c385, that is independent of [NADH]:

$$F_c385 = F385 - F456 \cdot Slope \quad (A4a)$$

Substitution of F385 and F456 in Eq. A4a, using Eqs. A1 and A2, respectively and slope = A_{385}/A_{456}, demonstrates that F_c385 is independent of [NADH]:

$$F_c385 = (BG_{385} - BG_{456} \cdot A_{385}/A_{456}) \cdot m(t) \quad (A4b)$$

Provided that the non-NADH-dependent fluorescence and quantum yields are constant, F_c385 provides a constant reference signal that is only modulated by the motion artifact. A corrected fluorescence ratio, $Ratio^c$, may then be calculated according to:

$$Ratio^c = F456/F_c385 = a + b \cdot [NADH] \quad (A5a)$$

where

$$a = BG_{456}/(BG_{385} - BG_{456} \cdot A_{385}/A_{456}) \quad (A5b)$$

$$b = A_{456}/(BG_{385} - BG_{456} \cdot A_{385}/A_{456}) \quad (A5c)$$

Equation A5 demonstrates that the fluorescence ratio is linearly dependent on [NADH] with slope b, and intercept a. The NADH/NAD^+ ratio during control condition is defined as:

$$NADH/NAD^+ = \quad (A6)$$

$$(NADH_{ctrl} - NADH_{min}) / (NADH_{max} - NADH_{min})$$

where $NADH_{ctrl}$ is [NADH] during control conditions, $NADH_{min}$ is maximally oxidized [NAD^+] and $NADH_{max}$ is maximally reduced [NAD^+]. In terms of $Ratio^c$ (Eq. A5a, and assuming that a and b are constant during NADH calibration):

$$NADH/NAD^+ = \quad (A7)$$

$$(Ratio^c_{ctrl} - Ratio^c_{min}) / (Ratio^c_{max} - Ratio^c_{min})$$

We thank Dr. Peter Backx for help with the design of the muscle chamber and trabecula preparation methods. This work was supported in part by the American Heart Association, Metropolitan Chicago, grant-in-Aid (RB) and by National Institute of Health HL30077 and HL52478 (DMB).

REFERENCES

Ashruf, J. F., J. M. C. C. Coremans, H. A. Bruining, and C. Ince. 1995. Increase of cardiac work is associated with decrease of mitochondrial NADH. *Am. J. Physiol.* 269:H856–H862.

Backx, P. H., and H. E. Ter Keurs. 1993. Fluorescent properties of rat cardiac trabeculae microinjected with fura-2 salt. *Am. J. Physiol.* 264: H1098–H1110.

Balaban, R. S., and F. W. Heineman. 1989. Control of mitochondrial respiration in the heart in vivo. *Mol. Cell. Biochem.* 89:191–197.

Balaban, R. S., and L. J. Mandel. 1988. Metabolic substrate utilization by rabbit proximal tubule. An NADH fluorescence study. *Am. J. P.* 254: F407–F416.

Bassani, J. W., R. A. Bassani, and D. M. Bers. 1993. Ca^{2+} cycling between sarcoplasmic reticulum and mitochondria in rabbit cardiac myocytes. *J. Physiol.* 460:603–621.

Brandes, R., V. M. Figueredo, S. A. Camacho, B. M. Massie, and M. W. Weiner. 1992. Suppression of motion artifacts in fluorescence spectroscopy of perfused hearts. *Am. J. Physiol.* 263:H972–H980.

Brandes, R., V. M. Figueredo, S. A. Camacho, and M. W. Weiner. 1994. Compensation for changes in tissue light absorption in fluorometry of hypoxic perfused rat hearts. *Am. J. Physiol.* 266:H2554–H2567.

Chance, B., J. R. Williamson, D. Jamieson, and B. Schoener. 1965. Properties and kinetics of reduced pyridine nucleotide fluorescence of the isolated and in vivo rat heart. *Biochem. Z.* 341:357–377.

Chapman, J. B. 1972. Fluorometric studies of oxidative metabolism in isolated papillary muscle of the rabbit. *J. Gen. Physiol.* 59:135–154.

Cooper, G., 1979. Myocardial energetics during isometric twitch contractions of cat papillary muscle. *Am. J. Physiol.* 236:H244–H253.

Crompton, M. 1990. The role of Ca^{2+} in the function and dysfunction of heart mitochondria. *In* Calcium and the Heart. G. A. Langer, editor. Raven Press Ltd., New York. 167–199.

Di Lisa, F., G. Gambassi, H. Spurgeon, and R. G. Hansford. 1993. Intramitochondrial free calcium in cardiac myocytes in relation to dehydrogenase activation. *Cardiovasc. Res.* 27:1840–1844.

Doumen, C., B. Wan, and O. Ondrejickova. 1995. Effect of BDM, verapamil, and cardiac work on mitochondrial membrane potential in perfused rat hearts. *Am. J. Physiol.* 269:H515–H523.

Eng, J., R. M. Lynch, and R. S. Balaban. 1989. Nicotinamide adenine dinucleotide fluorescence spectroscopy and imaging of isolated cardiac myocytes. *Biophys. J.* 55:621–630.

Estabrook, R. W., J. Gonze, and S. P. Nissley. 1963. A possible role for pyridine nucleotide in coupling mechanism of oxidative phosphorylation. *Fed. Proc.* 22:1071–1075.

Fossel, E. T., H. E. Morgan, and J. S. Ingwall. 1980. Measurement of changes in high-energy phosphates in the cardiac cycle using gated 31P nuclear magnetic resonance. *Proc. Natl. Acad. Sci. (USA).* 77: 3654–3658.

Fralix, T. A., F. W. Heineman, and R. S. Balaban. 1990. Effects of tissue absorbance on NAD(P)H and Indo-1 fluorescence from perfused rabbit hearts. *FEBS Lett.* 262:287–292.

From, A. H., M. A. Petein, S. P. Michurski, S. D. Zimmer, and K. Ugurbil. 1986. 31P-NMR studies of respiratory regulation in the intact myocardium. *FEBS Lett.* 206:257–261.

From, A. H., S. D. Zimmer, S. P. Michurski, P. Mohanakrishnan, V. K. Ulstad, W. J. Thoma, and K. Ugurbil. 1990. Regulation of the oxidative phosphorylation rate in the intact cell. *Biochemistry.* 29:3731–3743.

Hansford, R. G. 1991. Dehydrogenase activation by Ca2+ in cells and tissues. [Review]. *J. Bioenerg. Biomembr.* 23:823–854.

Heineman, F. W., and R. S. Balaban. 1993. Effects of afterload and heart rate on NAD(P)H redox state in the isolated rabbit heart. *Am. J. Physiol.* 264:H433–H440.

Jacobus, W. E., R. W. Moreadith, and K. M. Vandegaer. 1982. Mitochondrial respiratory control. Evidence against the regulation of respiration by extramitochondrial phosphorylation potentials or by [ATP]/[ADP] ratios. *J. Biol. Chem.* 257:2397–2402.

Ji, S., B. Chance, K. Nishiki, T. Smith, and T. Rich. 1979. Micro-light guides: a new method for measuring tissue fluorescence and reflectance. *Am. J. Physiol.* 236:C144–C156.

Kantor, H. L., R. W. Briggs, K. R. Metz, and R. S. Balaban. 1986. Gated in vivo examination of cardiac metabolites with 31P nuclear magnetic resonance. *Am. J. Physiol.* 251:H171–H175.

Katz, L. A., A. P. Koretsky, and R. S. Balaban. 1987. Respiratory control in the glucose perfused heart. A 31P NMR and NADH fluorescence study. *FEBS Lett.* 221:270–276.

Kobayashi, K., and J. R. Neely. 1983. Mechanism of pyruvate dehydrogenase activation by increased cardiac work. *J. Mol. Cell. Cardiol.* 15:369–382.

Koretsky, A. P., L. A. Katz, and R. S. Balaban. 1987. Determination of pyridine nucleotide fluorescence from the perfused heart using an internal standard. *Am. J. Physiol.* 253:H856–H862.

Koretsky, A. P., S. Wang, J. Murphy-Boesch, M. P. Klein, T. L. James, and M. W. Weiner. 1983. ^{31}P NMR spectroscopy of rat organs, in situ, using chronically implanted radiofrequency coils. *Proc. Natl. Acad. Sci. (USA).* 80:7491–7495.

Laughlin, M. R., and F. W. Heineman. 1994. The relationship between phosphorylation potential and redox state in the isolated working rabbit heart. *J. Mol. Cell. Cardiol.* 26:1525–1536.

McCormack, J. G., A. P. Halestrap, and R. M. Denton. 1990. Role of calcium ions in regulation of mammalian intramitochondrial metabolism. [Review]. *Physiol. Rev.* 70:391–425.

Scott, D. A., L. W. Grotyohann, J. Y. Cheung, and R. C. Scaduto, Jr. 1994. Ratiometric methodology for NAD(P)H measurement in the perfused rat heart using surface fluorescence. *Am. J. Physiol.* 267:H636–H644.

Snow, T. R., and P. B. Bressler. 1977. Oxygen sufficiency in working rabbit papillary muscle at 25 degrees C. *J. Mol. Cell. Cardiol.* 9:595–604.

White, R. L., and B. A. Wittenberg. 1993. NADH fluorescence of isolated ventricular myocytes: effects of pacing, myoglobin, and oxygen supply. *Biophys. J.* 65:196–204.

Yasumura, Y., T. Nozawa, S. Futaki, N. Tanaka, and H. Suga. 1989. Time-invariant oxygen cost of mechanical energy in dog left ventricle: consistency and inconsistency of time-varying elastance model with myocardial energetics. *Circ. Res.* 64:764–778.